Preprints, 10th IFAC International Symposium on
Advanced Control of Chemical Processes
Shenyang, Liaoning, China, July 25-27, 2018

Dynamic Optimization and Control of Chemical Looping Combustion Combined Cycle Power Plants ⋆

Lu Han * Chen Chen * George M. Bollas *

* Department of Chemical & Biomolecular Engineering, University of Connecticut, Storrs, CT 06269 USA (e-mail: george.bollas@uconn.edu).

Abstract: Integration of combined cycle (CC) with chemical-looping combustion power plants (CLC) is studied for its potential for high power plant efficiency and low-cost CO_2 capture. Dynamic modeling of the integrated process is used as a tool to analyze the extrema of CLC-CC power plant efficiency. Specifically, this work proposes control architectures for the CLC reactor and the integrated power plant. The time-averaged optimal CLC-CC power plant efficiency is estimated at 51.84% with CO_2 capture efficiency at 96%. The main factor that limits the CLC-CC power plant efficiency is the reactor temperature, which is constrained by the oxygen carrier material. Plant-level sensitivity analysis shows that the inlet air temperature at the heat removal stage and gas compressor/gas turbine pressure ratio are the most important operating variables and if properly tuned the CLC-CC power plant can reach efficiencies sufficiently high for its economic deployment as a carbon neutral power generation option.

Keywords: chemical looping combustion, combined cycle power plants, dynamic optimization, control.

1. INTRODUCTION

Global warming due to greenhouse gas emissions, particularly CO_2 from fossil fuel combustion in power plants, is a major concern globally. An international agreement was reached to maintain the global temperature increase below 2 °C with respect to pre-industrial levels (Nordhaus, 2010). This requires that the concentration of CO_2 in the atmosphere is lower than 450 vppm, which in the future can be accomplished with incorporation of renewable sources with low carbon content, such as solar, wind, hydropower, geothermal energy and biomass, into the energy system. However, fossil fuels continue to provide most of the world's energy. For instance, reference case projections in the annual energy outlook reported by the U.S. Energy Information Administration (EIA), show that fossil fuels in the U.S. are still the dominant energy source and will provide more than 76.6% of the total energy production until 2050 (EIA, 2018). Thus, other options for reducing CO_2 emissions have drawn attention, such as CO_2 capture and storage (CCS) technologies and reducing fossil fuel combustion by improving power plant efficiency (Rubin et al., 2007). Natural gas and coal provide ∼50% of the world's electricity needs. Because coal is a fuel that is abundant, inexpensive, safely stored and transported, the power plants fueled by coal still provide ∼40% of world's electricity EIA (2018). However, the combustion of coal emits harmful gases, such as sulfuric acids, arsenic and ash. Compared to coal, natural gas is a cleaner fuel due to its lower content in impurities and higher combustion efficiency. Specifically, power plants fueled by natural gas release ∼40% less CO_2 than coal-fired power plants (de Gouw et al., 2014). The U.S. coal consumption is projected to decline through 2050, while natural gas consumption in the electric power sector is substantially increasing (EIA, 2018). Natural gas is projected to serve as the mid-term solution to the transition from fossil-fueled power plants to a renewable electricity infrastructure.

Conventional CCS technologies typically consist of separation, compression, transport and storage steps, which are energy intensive and penalize power plant efficiency by 7−14% (Johansson et al., 2006; Bolland and Undrum, 2003). To address CCS efficiency issues, chemical-looping combustion (CLC) has been proposed as a novel and efficient process for producing energy and capturing CO_2, with the potential to reduce the cost of CO_2 capture by 50% (Hossain and de Lasa, 2008). Adanez et al. (2012) reported that the cost of CO_2 capture per tonne is 7.1-15 dollars for CLC, when it is 21.3-43.8 dollars for a pre-combustion technology using integrated gasification combined cycles, and 15.4-35.5 dollars for an oxy-fuel process. In the CLC process, CO_2 is inherently separated from N_2, which limits the need for additional process equipment and reduces the energy penalty for the separation of CO_2. The fuel and air are unmixed by use of a metal oxide as oxygen carrier (OC) to transport oxygen from the air reactor, where the OC is oxidized by air, to the fuel reactor, where the OC is reduced by fuel. Moreover, combined cycle (CC) power plants can reach efficiencies of up to ∼60%,

⋆ This material is based upon work supported by the National Science Foundation under Grant No. 1054718. This work was partially sponsored by the United Technologies Corporation Institute for Advanced Systems Engineering (UTC-IASE) of the University of Connecticut. Any opinions expressed herein are those of the authors and do not represent those of the sponsor.

which is by far the highest efficiency in thermal power processes (Kehlhofer et al., 2009). Therefore, the solution to environmental concerns of the power generation sector, should include (in the short term) CC power plants for their capability to reduce CO_2 emissions per unit of energy produced. Integration of CLC and CC is, therefore, the most promising approach, in terms of efficiency and CO_2 capture potential.

System-level dynamic simulation and optimization can play a significant role in exploring the feasibility to integrate CLC reactors with CC power plants. For example, Chen et al. (2016) presented a dynamic model capturing the dynamics of CLC-CC power plants with carbon footprint constraints. Their simulation showed that the CLC-CC power plant can generate a stable power output, only slightly affected by the intrinsic dynamics of the semi-batch operation of its fixed bed CLC reactors. Spallina et al. (2014) simulated large-scale coal gasification-based power cycles with fixed bed CLC reactors. Naqvi and Bolland (2007) simulated a natural gas fired CLC-CC power plant with CO_2 compression. CC power plants integrating an island of batch, fixed bed CLC reactors operating in parallel, are a promising and feasible process option, with estimated performance reported to reach efficiencies of up to 50% at 96% CO_2 capture. In prior work, we focused on exploring the theoretical feasibility of integrating CLC with CC, and presented a modeling framework to estimate the static and dynamic performance of a CC power plant, powered by semi-batch fixed-bed CLC reactors, fueled with natural gas (Chen et al., 2016). The plant model with a simple control design was simulated and validated against full load data reported in the literature. The conventional combustor was replaced with a high-pressure fixed-bed CLC island, which was optimized to improve the overall plant efficiency by the utilization of gas streams from CLC reactors. Moreover, the CC power plant was only slightly affected by the intrinsic batch-type operation of fixed bed reactors. The estimated efficiency of the CLC-CC power plant was ~48% with small fluctuations of ~2% around the desired steady state. The relatively stable power output was accomplished by optimizing the CLC's operational strategy.

The organization of this paper follows the description of each sub-model. In the first section, the design assumptions and optimal control structure of the CLC reactor system are presented. Secondly, the combined cycle power plant model is discussed, focusing on the optimal integration with CLC and plant-wide design and control for efficiency optimization. The efficiency benefits of applying advanced control to streamline the design and integration of CLC with a combined cycle are discussed.

2. DESCRIPTION OF THE CLC-CC PROCESS

In a typical CC power plant, the combustion of fuel and compressed air generates high-temperature flue gas, which is expanded in the gas turbine to produce electricity. The hot exhaust gas from the gas turbine is utilized in a heat recovery steam generator (HRSG) to generate superheated steam, which is used to produce additional electricity in a steam cycle. In this work, the configuration and data of a CC power plant located in Monterrey were used. The reference CC power plant with power output of 250 MW and net efficiency of ~57.9%, includes a 160 MW ABB GT 24 gas turbine, an ABB CE once-through, supercritical HRSG, and a 90 MW ABB reheat steam turbine unit (Chen et al., 2016). The natural gas feeding the conventional combustor is compressed to a high pressure of 30 bar. The hot gas from the topping gas turbine feeds the bottoming steam cycle to transfer heat to the water circuit. The superheated steam at 160 bar and 565 °C is expanded in multi-stage steam turbines to generate electricity. The detailed steps of modeling and validation of the power plant model are given in Chen et al. (2016). Figure 1 presents the diagram of a CC power plant integrated with fixed bed CLC reactors. Compared with the arrangement of the CLC-CC power plant presented in prior work (Chen et al., 2016), this CLC-CC power plant design was modified to improve plant efficiency. The stream of N_2 from the purge stage was used as secondary heat removal (HR2, noted as stream (13)) to superheat the steam (noted as stream (20)) from the HRSG1 to the HRSG3. Moreover, the gas from the oxidation stage (noted as stream (4)) was first fed to the HRSG4 to superheat the steam (noted as stream (21)) from the HRSG3, then the high pressure depleted air (noted as stream(5)) was used to preheat the air from the air compressor, and finally it was mixed with the air fed to the HR1 phase. This arrangement employed two more HRSGs (HRSG3 and HRSG4) than the previous design to utilize the heat of the purge streams and the heat of the depleted air from the oxidation stage.

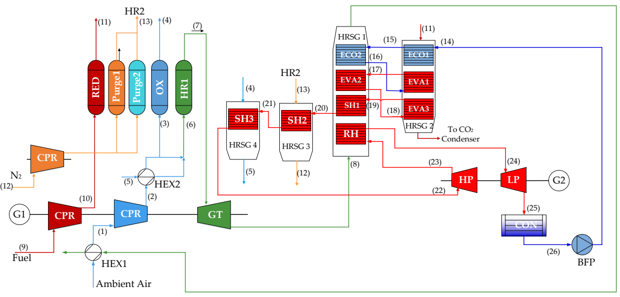

Fig. 1. Diagram of the optimal CC power plant with fixed bed CLC reactors. (CPR: Compressor; G: Power Generator; GT: Gas Turbine; SH: Superheater; RH: Reheater; EVA: Evaporator; ECO: Economizer; HP: High-pressure Turbine; LP: Low-pressure Turbine; CON: Condenser.

3. CLC OPTIMAL CONTROL FORMULATION

Integration of CLC with CC power plants can be accomplished if the CLC reactor operates at high pressure. While there have been studies on the feasibility of interconnected fluidized bed CLC reactors operating at high pressure, it is challenging to maintain stable solids circulation under pressurized conditions, while oxygen carrier attrition is an additional concern. Fixed bed CLC reactor designs mitigate the challenge of operating at high pressure, but create new operational challenges due to their inherent batch-type operation. The oxygen carrier is static and alternating flows of fuel and air pass through the bed in order to reduce and oxidize the oxygen carrier. These reactions are kinetically controlled and have different reaction enthalpies. Thus, the exhaust temperature of the CLC reactor changes dramatically as the cycle switches between reduction and oxidation. In the works(Hamers et al., 2013), a control strategy that balances the reduction and oxidation conditions was found necessary to achieve a suitable fixed bed CLC operation for the combined cycle. The main challenge is maintaining a constant high-temperature gas stream to feed the downstream gas turbine, while consistently meeting the constraints on CO_2 capture efficiency, pressure drop, and fuel conversion.

The general concept in this work, is to design multiple fixed bed reactors operating in parallel in order to process a continuous stream of fuel and air. One approach is to simultaneously optimize the design of a network of CLC reactors. However, due to the extreme computational cost, we sought a more practical approach, which was to optimize the operation of a single CLC reactor and then apply the optimal process to a series of identical reactors, with a predetermined time delay. For given power requirement and oxygen carrier, an optimal control strategy was implemented to seek the CLC decision variables that maximize a metric of energy efficiency of the fixed bed while satisfying the dynamic constraints at all times (Han and Bollas, 2016b,a). These decision variables include the time duration at which the reactor is undergoing reduction and oxidization, the temperature and flow rate of the inlet air and fuel, and oxygen carrier properties (e.g., active loading of the metal oxide), as summarized in Table 1. It is noted that the control profile for the feed gas is modeled using piecewise constant functions, represented as $\mathbf{u}(\tau_i) = \mathbf{u}_i$, where $\mathbf{u}$ is the vector of temperature, flow, and composition of the gas stream and τ_i is the time duration of the i-th CLC step, i.e., reduction, purge, and oxidation. The heat removal stage is the useful part of the oxidation cycle, wherein the heat liberated from the exothermic oxidation reaction is removed from the bed by gas convection. This high-temperature air stream is expanded in the gas turbine of the combined cycle, while the other low-quality streams are sent to steam cycle. The set of control variables is summarized in the design vector, $\boldsymbol{\phi}$, shown in (1), which is constrained by upper and lower limits permitted in the design space, $\boldsymbol{\Phi}$:

$$\boldsymbol{\phi} = [\boldsymbol{u}_i, \tau, \omega]. \tag{1}$$

Table 1. Control variables in the optimal control problem.

Control variables	Notation
Air feed rate	$\mathbf{u}_i$
Air temperature	-"-
Fuel feed rate	-"-
Reduction time interval	τ_i
Oxidation time interval	-"-
Heat removal time interval	-"-
Metal oxide content in oxygen carrier	$\boldsymbol{\omega}$

3.1 Optimization Problem

The objective of the optimal control problem is to maximize an efficiency of the CLC power generation capability over the cyclic steady-state operation of the fixed bed. One metric of the energy efficiency is presented in (2), as the fraction of the total exhaust gas enthalpy feeding the gas turbine (Han and Bollas, 2016b,a):

$$\eta_{HR} = \frac{\int_{t_0}^{\tau_{HR}\ \ 1} \left(\dot{m}_{out}(t) h_{out}(t)\right) dt}{\int_{t_0}^{\tau_{cycle}} \left(\dot{m}_{out}(t) h_{out}(t)\right) dt}, \tag{2}$$

where $T_{out}, \dot{m}_{out}, h_{out}$ are the temperature, mass flow rate, and enthalpy of the exhaust stream, τ_{HR} is the time duration of heat removal to produce electricity in the gas turbine, and τ_{cycle} is the time interval for one complete redox cycle. Maximization of the heat removal efficiency of the CLC unit (2) directly benefits the efficiency for the power generation sector. It is also necessary to take into account the trade-off of efficiency in order to have sufficient CO_2 capture. Typical ranges for CLC processes are $\geq 96\%$ CO_2 capture efficiency and $\geq$ 98% fuel conversion, as written in (3) and (4). Additional constraints to maintain a stable $T_{out}(t)$ during heat removal (within a set tolerance, δ from the turbine inlet temperature set-point, TIT), reasonable pressure drop across the reactor, and maximum allowable internal temperature should be incorporated, as written in (5) and (7):

$$S_{CO_2}(t) = \frac{\int_{t_0}^{\tau_{RED}} F_{out}(CO_2, t) dt}{\int_{t_0}^{\tau_{RED}} F_{in}(CH_4, t) dt} \geq 96\%, \tag{3}$$

$$X_{fuel}(t) = 1 - \frac{\int_{t_0}^{\tau_{RED}} F_{out}(CH_4, t) dt}{\int_{t_0}^{\tau_{RED}} F_{in}(CH_4, t) dt} \geq 98\%, \tag{4}$$

$$TIT - \delta \leq T_{out}(t) \leq TIT + \delta, \tag{5}$$

$$\frac{\Delta P}{P_{in}(t)} \leq \Delta P^{max}, \tag{6}$$

$$T(t, z) + \delta \leq T^{max}. \tag{7}$$

The optimal control problem can, then, be formulated as follows:

$$\begin{aligned}
&\max_{\boldsymbol{\phi}} \eta_{HR}(t) \\
&\quad \text{Subject to} \\
&\qquad\qquad \text{Eqs. } (3-7) \\
&\qquad\qquad \mathrm{f}\big(\dot{\mathrm{x}}(t), \mathrm{x}(t), \mathrm{u}(t), \theta, t\big) = 0, \\
&\qquad\qquad \mathrm{f}_0\big(\dot{\mathrm{x}}_0, \mathrm{x}_0, \mathrm{u}_0, \theta, t_0\big) = 0, \\
&\qquad\qquad \mathrm{y}(t) = \mathrm{h}\big(\mathrm{x}(t)\big), \\
&\qquad\qquad \mathrm{x}^{min} \leq \mathrm{x} \leq \mathrm{x}^{max} \\
&\qquad\qquad \mathrm{u}_i^{min} \leq \mathrm{u}_i \leq \mathrm{u}_i^{max} \qquad\qquad \forall i \in [1, N_u] \\
&\qquad\qquad \tau_i^{min} \leq \tau_i \leq \tau_i^{max} \qquad\qquad \forall i \in [1, N_u] \\
&\qquad\qquad \omega^{min} \leq \omega \leq \omega^{max}
\end{aligned} \tag{8}$$

In (8), f is the set of DAEs describing the CLC reactions and hydrodynamics inside a fixed bed reactor (Han and Bollas, 2016b), with its initial conditions and constraints for states x, admissible inputs $\mathrm{u_i}$, cycle times τ_i and metal oxide content in the oxygen carrier ω. Since it normally takes more than 1 redox cycle to reach cyclic steady-state, the time horizon of the optimization was set to at least 2 times the τ_{cycle}. By using an extended time horizon, a periodicity condition was ensured in the optimization problem. The above problem was implemented and solved in the commercial software package gPROMS (Process Systems Enterprise, 2017).

3.2 Case study: Fixed bed CLC with NiO and methane

To demonstrate the proposed optimal control formulation, a case study of a Ni-based CLC carried out in a fixed bed reactor is presented. The design parameters for the CLC system were calculated to meet the requirements of a 250 MW combined cycle power plant. Table 2 shows the specific requirements for a single fixed bed reactor.

Table 2. Fixed bed CLC reactor parameters.

Parameter	Value
Active weight content of metal oxide	40 wt.% NiO
Particle diameter	5 mm
Reactor length	9.4 m
Reactor diameter	4.7 m
Max. pressure drop	0.03 bar
CH_4 flow rate	8.626 kg/s
Purge gas	100% N_2
Max. reactor temperature	1300 °C
Max. reactor pressure	30 bar
Turbine inlet temperature, TIT	1250 °C
Temperature tolerance, δ	50 °C

The optimization procedure was carried out using the constraints (4-7), where η_{HR} was expressed with (2). Figure 2 shows the temperature, enthalpy, and selectivity of the exhaust stream at the optimized cyclic steady-state operation. As shown, the oxidation step generates a high-temperature air stream, which achieves the desired set-point with minimal deviations. The heat removal step initiates when the exhaust temperature is within δ from TIT. After much of the heat has exited the bed and $T_{out}(t) < TIT - \delta$, the reactor is then briefly purged and the feed switches to fuel. The flow rate of the fuel is much lower compared to air, which explains the sudden drop in exhaust gas enthalpy. The reduction exhaust shows a high conversion of CH_4 to CO_2 and H_2O and very minor amounts of syngas and unconverted fuel before switching to purge and oxidation. In Figure 2(c), there is a sudden drop in O_2 and rise in N_2 when the cycle switches from oxidation (OX) to heat removal (HR) because the exhaust gas from oxidation was mixed with inlet air during HR, in an effort to recycle the gas streams and improve overall energy efficiency.

As shown from this example, the desired temperature profiles and CO_2 selectivity can be achieved by solving an optimal control problem of the fixed bed CLC operation. The dynamic features of Figure 2 are less pronounced when we simulate multiple instances of the same reactor operating in parallel. In particular, the hot gas feeding the gas turbine experiences an overall temperature fluctuation of $< 50°C$ for this example. The properties of the mixed CLC exhaust are used as boundary conditions into the combined cycle power plant, as discussed in the following section.

3.3 Optimal CLC-CC power plant performance

Integration of the CLC island in the CC power plant required the use of five reactors in parallel, in order to deliver continuous conversion of the fuel feed. The number of reactors was calculated on the basis of total cycle time (3664 sec) divided by the reduction time (750 sec), shown in Figure 2. The exhaust gas from each reactor was mixed according to its originating cycle. Thus, the overall exhaust of the CLC island was grouped as: CO_2/H_2O from reduction, N_2/O_2 from oxidation, air from the first heat removal (HR1), and N_2 from purge (as the second heat removal, HR2). The properties of the mixed gas streams downstream the CLC reactor network were used as boundary conditions to the power plant. The combined cycle power plant model, developed in Dymola (Elmqvist et al., 1996), included heat exchangers preheating air to the CLC island, gas turbine and compressor, and steam cycle sub-models, as shown in Figure 3. Figure 3(a) shows that the oxidation exhaust gas (noted as stream (5) in Figure 1) from the HRSG3 was applied to preheat the air from the gas compressor to the oxidation phase. Then, this oxidation exhaust gas stream was mixed with the air from the gas compressor and the mixture fed the HR1 CLC phase. As shown in Figure 3(b), the preheated air was pressurized by the air compressor, and the heat of the HR1 exhaust gas was transferred to mechanical torque through the gas turbine. The properties of the gas turbine exhaust, CO_2/H_2O from reduction, N_2/O_2 from oxidation, and N_2 from HR2 were used as boundary conditions to the steam cycle sub-model, as shown in Figure 3(c). Four HRSGs were used in the steam cycle model to utilize the heat of the exhaust from reduction, HR2, oxidation, and gas turbine. The PID controller was used for manipulating the pump speed to control the water flow in the steam cycle as shown in Figure 3(c). A reheater was used to re-superheat the steam after expansion in the HP turbine. The steam was condensed to liquid phase in the condenser and the water was fed back to the pump to close the loop. For simplification, multiple-stage heaters, turbines, condensers and pumps were grouped according to their functions in

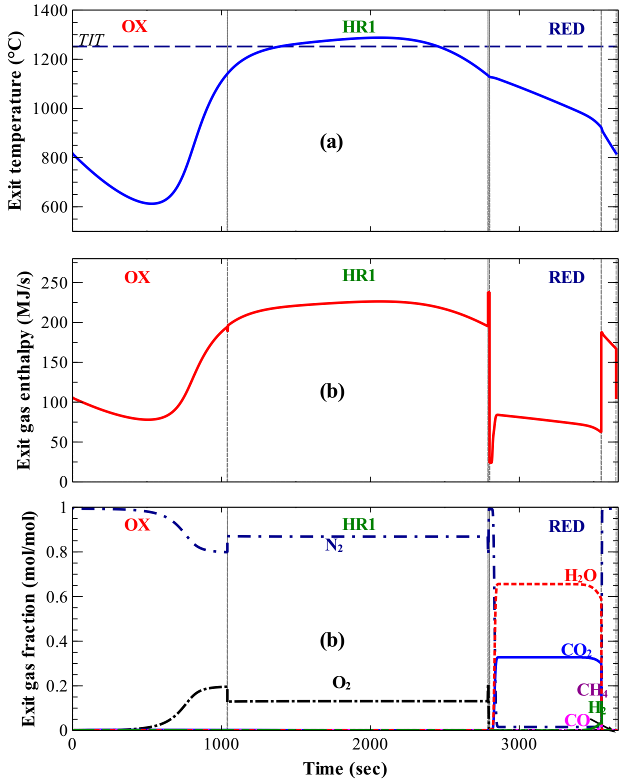

Fig. 2. Simulation results of the Ni-based fixed bed reactor using parameters from Table 2.

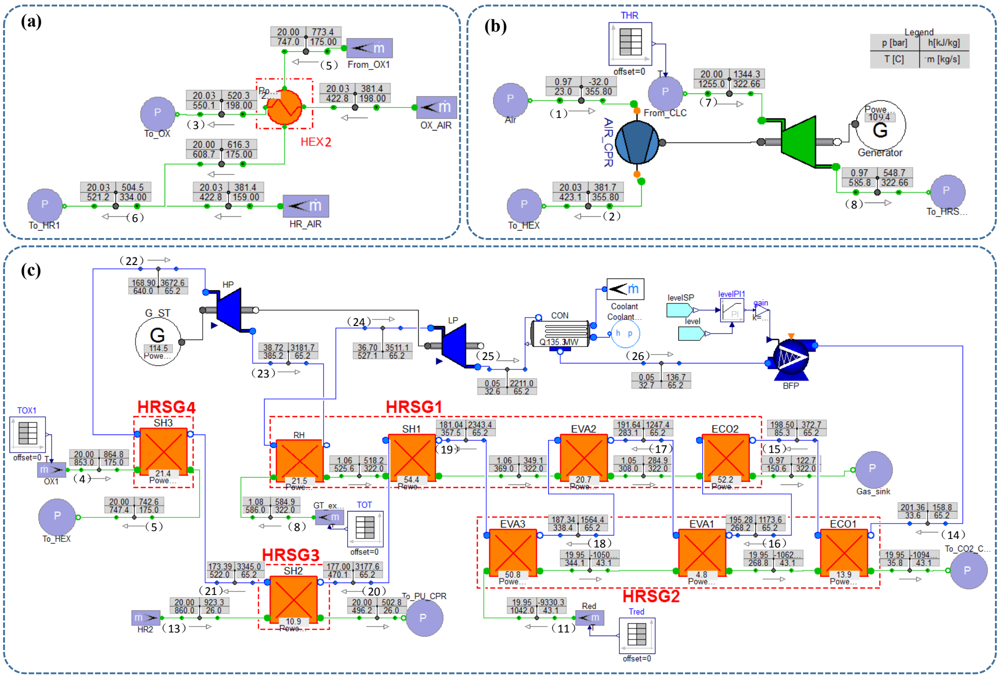

Fig. 3. Diagram of the Dymola model of the CLC-CC power plant: (a) air preheater model; (b) gas turbine model; (c) steam cycle model. (Numbers in parentheses correspond to streams shown in Figure 1)

the model developed. For example, the heaters used to superheat steam in HRSG1 were grouped as SH1 as shown in Figure 3(c), for brevity.

The temporal profiles of the mixed gas stream properties are shown in Figure 4(a). The fluctuation of the gas turbine inlet temperature is smaller than that of one CLC reactor (Figure 2(a)) because of the mixing of the exhaust of five reactors that operate in parallel. Specifically, the gas turbine fed to HRSG1 has an average temperature of 586 °C and mass flow rate of 322.5 kg/s. The reduction exhaust fed to HRSG2 had an average temperature of 1042 °C and mass flow rate of 43.1 kg/s, the oxidation exhaust fed to HRSG3 had an average temperature of 853 °C and mass flow rate of 175 kg/s, and the HR2 exhaust fed to HRSG4 had an average temperature of 860 °C and mass flow rate of 26 kg/s. As can be seen in Figure 4(a), there is a small deviation from ideal periodicity in the reduction exhaust temperature profile. This is because two of the five reactors are in reduction phase for 100 sec after every complete redox interval. Figure 4(b) shows the temporal profiles of power generation by the gas turbine and steam turbine, and total power generation. The power generated by the gas turbine, corresponds to the fluctuating temperature profile of gas turbine inlet, also oscillates over time and has an average of 109 MW with a standard deviation of 2.38 MW. The power generated by the steam turbines, which responds to the fluctuating temperature profile of gas turbine outlet, reduction exhaust and oxidation exhaust. It fluctuates over time with an average of 114.6 MW and a standard deviation of 1.90 MW. The total power fluctuates over time with an average of 223.6 MW and deviation of 3.88 MW. The boiler feed pump is controlled by a PID controller, which manipulates the pump speed to regulate the mass flow rate of water circulating in the steam cycle.

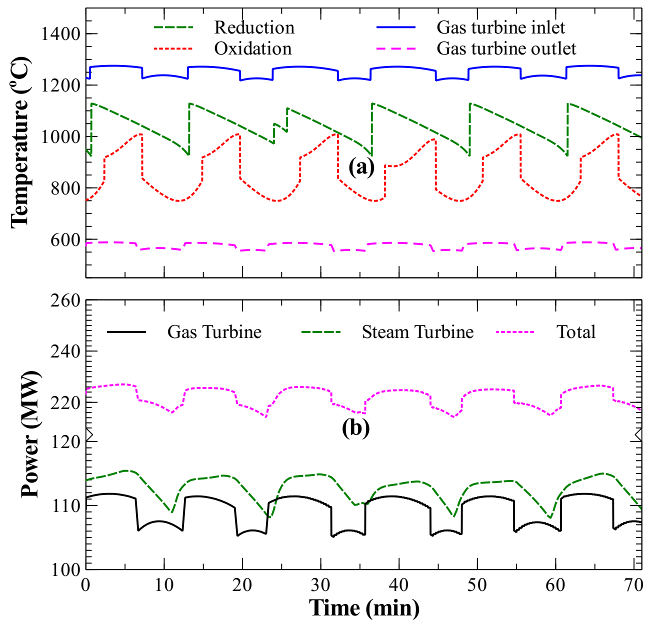

Fig. 4. Temperature profiles of (a) the gas streams in terms of reduction exhaust, oxidation exhaust, gas turbine inlet gas, gas turbine exhaust; (b) power generations by gas turbine and steam turbine and the total power generation.

3.4 Comparison of reference power plant and optimal CLC-CC power plant

Table 3 presents the detailed comparison of the Monterrey CC power plant and the optimal CLC-CC power plant. The optimal CLC-CC has CO_2 capture efficiency of 96% and optimal power plant efficiency of 51.84%, which is consistent with the CLC-CC power plant efficiencies reported in previous work (Chen et al., 2017). This efficiency is ∼6% points lower than the reference power plant. The mass flow rate of CO_2 after the reduction (stream (11) in Figure 1) is only 23.72 kg/s. If the CO_2 is compressed to 110 bar after the condensation of water at 30 °C, it will take ∼3 MW for the compression, thus the efficiency will drop to 51.14%. Compared with the reference power plant of Chen et al. (2016), the optimal CLC-CC power plant has higher power generation by 114.6 MW from the steam cycle, while lower power generation by 108 MW from the gas turbine. The difference in power contributions by the Brayton and Rankine cycles is due to the heat management strategies, which also affect the maximum net electricity efficiency, as presented in the work by Spallina et al. (2014). The lower TIT is a contributor to the efficiency loss according to the work by Naqvi and Bollad Naqvi and Bolland (2007), but TIT is constrained by the OC material.

Table 3. Comparison of Monterrey CC and optimal CLC-CC power plants.

Power plant	Monterrey CC	Optimal CLC-CC
Fuel	Natural gas	Methane
Fuel input [MW]	431.3	431.3
Fuel mass flow [kg/s]	8.784	8.626
Air mass flow [kg/s]	351	357
Ambient temperature [°C]	15	15
Air CPR inlet temperature [°C]	30	23
Ambient pressure [bar]	0.969	0.969
$\overline{TIT}$ [°C]	1440	1253
$\overline{TOT}$ [°C]	660	586
GT pressure ratio	30:1	20:1
GT exhaust mass flow [kg/s]	360	322.3
GT power [MW]	160	109
Steam mass flow [kg/s]	57	65.2
SH steam pressure [bar]	160	165
SH steam temperature [°C]	565	640
ST power [MW]	85.8	114.6
CO_2 capture efficiency [%]	0	96
Total power [WM]	250	223.6
Efficiency [%]	57.96	51.84

4. CONCLUSIONS

Chemical looping combustion was integrated with combined cycle power plant and their design configuration and control architecture were studied and optimized. Dynamic models of both processes were analyzed in an effort to understand what drives the efficiency of the integrated process. An optimal control strategy was designed for the CLC island and was integrated with an optimal design configuration for the integrated CLC-CC power plant. The estimated efficiency of 51.84% for an integrated, continuous power plant operating at CO_2 capture efficiency of 96% validates the status of chemical looping as one of the most promising future CCS technologies.

REFERENCES

Adanez, J., Abad, A., Garcia-Labiano, F., Gayan, P., and de Diego, L.F. (2012). Progress in Chemical-Looping Combustion and Reforming technologies. *Progress in Energy and Combustion Science*, 38(2), 215–282.

Bolland, O. and Undrum, H. (2003). A novel methodology for comparing CO2 capture options for natural gas-fired combined cycle plants. *Advances in Environmental Research*, 7(4), 901–911.

Chen, C., Han, L., and Bollas, G.M. (2016). Dynamic Simulation of Fixed-Bed Chemical-Looping Combustion Reactors Integrated in Combined Cycle Power Plants. *Energy Technology*, 4(10), 1209–1220.

Chen, C., Zhou, Z., and Bollas, G.M. (2017). Dynamic modeling, simulation and optimization of a subcritical steam power plant. Part I: Plant model and regulatory control. *Energy Conversion and Management*, 145, 324–334.

de Gouw, J.A., Parrish, D.D., Frost, G.J., and Trainer, M. (2014). Reduced emissions of CO 2 , NOx, and SO 2 from U.S. power plants owing to switch from coal to natural gas with combined cycle technology. *Earth's Future*, 2(2), 75–82.

EIA (2018). Annual Energy Outlook 2018 with projections to 2050. 1–64.

Elmqvist, H., Brück, D., and Otter, M. (1996). Dymola User's Manual.

Hamers, H., Gallucci, F., Cobden, P., Kimball, E., and van Sint Annaland, M. (2013). A novel reactor configuration for packed bed chemical-looping combustion of syngas. *International Journal of Greenhouse Gas Control*, 16, 1–12.

Han, L. and Bollas, G.M. (2016a). Chemical-looping combustion in a reverse-flow fixed bed reactor. *Energy*, 102, 669–681.

Han, L. and Bollas, G.M. (2016b). Dynamic optimization of fixed bed chemical-looping combustion processes. *Energy*, 112, 1107–1119.

Hossain, M.M. and de Lasa, H.I. (2008). Chemical-looping combustion (CLC) for inherent CO2 separationsa review. *Chemical Engineering Science*, 63(18), 4433–4451.

Johansson, E., Mattisson, T., Lyngfelt, A., and Thunman, H. (2006). Combustion of Syngas and Natural Gas in a 300 W Chemical-Looping Combustor. *Chemical Engineering Research and Design*, 84(9), 819–827.

Kehlhofer, R., Hannemann, F., Rukes, B., and Stirnimann, F. (2009). *Combined-Cycle Gas & Steam Turbine Power Plants*. PennWell, Tulsa, Oklahoma, 3rd edition.

Naqvi, R. and Bolland, O. (2007). Multi-stage chemical looping combustion (CLC) for combined cycles with CO2 capture. *International Journal of Greenhouse Gas Control*, 1(1), 19–30.

Nordhaus, W.D. (2010). Economic aspects of global warming in a post-Copenhagen environment. *Proceedings of the National Academy of Sciences*, 107(26), 11721–11726.

Process Systems Enterprise (2017). gPROMS, www.psenterprise.com/gproms, 1997-2017.

Rubin, E.S., Chen, C., and Rao, A.B. (2007). Cost and performance of fossil fuel power plants with CO2 capture and storage. *Energy Policy*, 35(9), 4444–4454.

Spallina, V., Romano, M., Chiesa, P., Gallucci, F., van Sint Annaland, M., and Lozza, G. (2014). Integration of coal gasification and packed bed CLC for high efficiency and near-zero emission power generation. *International Journal of Greenhouse Gas Control*, 27, 28–41.